JOURNAL OF GEOPHYSICAL RESEARCH, VOL. 107, NO. B1, 2006, 10.1029/2001JB000422, 2002

Crustal thicknesses in SE Brazilian Shield by receiver function analysis: Implications for isostatic compensation

Marcelo Assumpção

Institute of Astronomy, Geophysics, and Atmospheric Sciences, University of São Paulo, São Paulo, Brazil

David James

Department of Terrestrial Magnetism, Carnegie Institution of Washington, Washington D.C., USA

Arthur Snoke

Virginia Tech Seismological Observatory, Department of Geological Sciences, Virginia Polytechnical Institute and State University, Blacksburg, Virginia, USA

Received 14 June 2000; revised 30 January 2001; accepted 19 August 2001; published 10 January 2002.

[1] The Brazilian Lithosphere Seismic Project (BLSP, a joint project by University of São Paulo and Carnegie Institution, 1992–1999) operated more than 20 temporary broadband stations in the southeastern Brazilian shield. The area, a transect ~1000 km long and 300 km wide, covers different geological provinces: the Precambrian São Francisco craton, the adjacent Brasiliano (700–500 Ma) fold belts, and the Paraná basin of Paleozoic origin. Crustal thicknesses were estimated for 23 sites using receiver functions. For each station, receiver functions were stacked for different sets of earthquakes according to azimuth and distance. The *P*-to-*S* Moho converted phase was clearly identified at most sites. Crustal thicknesses were estimated using an average crustal *P* wave velocity of 6.5 km/s. Poisson's ratio of 0.23 ($Vp/Vs = 1.70$) was used for the São Francisco craton and adjacent fold belt (based on travel times from small, local earthquakes) and 0.25 was used for the Paraná basin and coastal belt. Crustal thicknesses ranged from 35–47 km. Although there is a clear inverse correlation between topography and Bouguer gravity anomalies in the study area, Moho depths show the opposite pattern from that expected: areas of low topography and less negative Bouguer anomalies, such as the Paraná basin, have thicker crust (40–47 km) compared with the high elevation areas of the craton and fold belt (37–43 km). Two hypothesis are proposed to explain the data: (1) A lower density, by 30–40 kg/m^3, in the lithospheric mantle under the Archean block of the São Francisco craton relative to the Proterozoic lithosphere is responsible for maintaining the high elevations in the plateau area. Relatively low density and high *P* wave velocity are compatible with a depleted (low FeO) composition for the Archean lithosphere. (2) Alternatively, if the density contrasts between Archean and Proterozoic lithospheres are smaller than the values above, then the crust beneath the Paraná basin must be more dense than that of the craton. Higher crustal density and high Poisson's ratio would be consistent with magmatic underplating in the lower crust beneath the Paraná basin, as inferred from other studies. *INDEX TERMS:* 7205 Seismology: Continental crust (1242); 9360 Information Related to Geographic Region: South America; 7218 Seismology: Lithosphere and upper mantle; *KEYWORDS:* crust, upper mantle, Brazil, Parana basin, San Francisco craton

1. Introduction: Brazilian Lithospheric Seismic Project (BLSP)

[2] A joint experiment between the University of São Paulo and Carnegie Institution of Washington, in collaboration with other institutions in Brazil and the United States, was undertaken in 1992 with the installation of up to 10 broadband stations in SE Brazil using STS-2 sensors and RefTek recorders. A description of the experiment with preliminary results were given by *James et al.* [1993] and *Snoke and James* [1997]. Figure 1 shows the stations occupied in the period 1992–1999 and the main geological provinces.

0148-0227/02/2001JB000422$09.00

[3] In the southern part of the São Francisco craton, an Archean block is preserved (ages from 2.5 to 3.2 Ga [*Teixeira and Figueiredo*, 1991]). The São Francisco craton is surrounded by Upper Proterozoic fold belts of the Brasiliano orogen (Brasília and Uruaçu belts), which was the last major tectonic event to amalgamate all crustal blocks into the present configuration. The Paraná basin started to develop in the early Paleozoic with subsidence thought to result from cooling of the whole region after the Brasiliano orogen [*Zalan et al.*, 1990]. On the basis of radiometric dates from two basement samples a Proterozoic "cratonic" nucleus was inferred beneath the Paraná basin [*Cordani et al.*, 1984; *Brito Neves and Cordani*, 1991]. The collision between this nucleus and the São Francisco craton resulted in a suture zone marked by a significant gravimetric gradient [*Lesquer et al.*, 1981], as shown by the dashed line in Figure 1 (also known as "Goiânia Flexure"). Extensive continental flood basalt was extruded on most of the Paraná basin, from 137 to 130 Ma, just prior to the South Atlantic

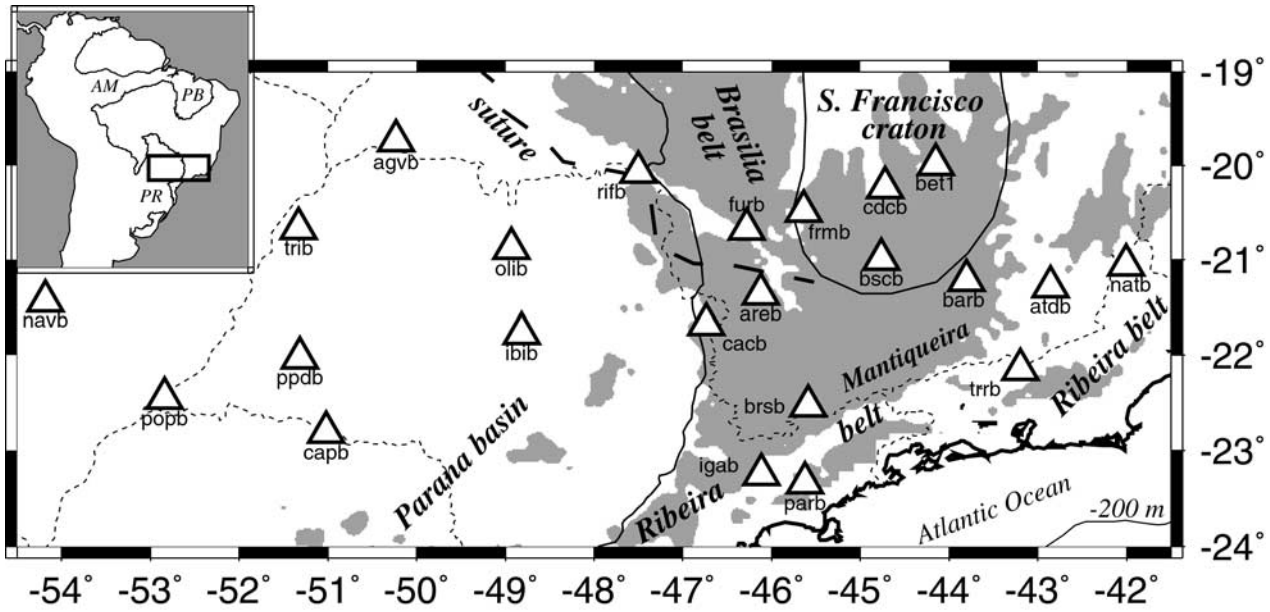

Figure 1. BLSP stations (triangles) and main geological units (delimited by thin solid lines) in SE Brazil. The Paleozoic Paraná sedimentary basin occupies the western part of the study area; the southern part of the São Francisco craton, with stations frmb, cdcb, and bscb, is characterized by Archean granitic-gneissic rocks. The shaded area shows elevations higher than 800 m, including the Serra da Mantiqueira plateau. The ''craton/plateau'' is defined here as the area enclosed by stations brsb, cacb, furb, bet1, and barb. The long dashed line labeled ''suture'' marks a steep gradient in the Bouguer anomalies (lower values in the Brasília fold belt and São Francisco craton) which has been interpreted as an Upper Proterozoic/lower Paleozoic suture between the São Francisco craton and a cratonic nucleus beneath the Paraná basin. The thin dashed lines are state boundaries. The inset shows the study area and the three main intracratonic basins of Paleozoic origin in South America: Amazon (AM), Parnaíba (PB), and Paraná (PR) basins.

opening. The source of this magmatism is usually attributed to a mantle plume related now to the Tristan da Cunha hot spot [*O'Connor and Duncan*, 1990; *Turner et al.*, 1994].

[4] Several techniques have been used with teleseismic events to estimate deep structure beneath the network, including body wave tomography, surface wave dispersion, and SKS splitting. A brief review of the main results so far are given below. The *P* and *S* wave tomography [*VanDecar et al.*, 1995] revealed two important results: (1) The first is a clear high-velocity root beneath the São Francisco craton, down to ~300 km depth and also an indication of high velocities beneath the central part of the Paraná basin. These results were consistent with the postulated cratonic block beneath the central part of the Paraná basin unaffected by the Brasiliano orogen [*Cordani et al.*, 1984; *Brito Neves and Cordani*, 1991]. (2) The second is a low-velocity column in the upper mantle, ~200 km wide extending from 200 to 600 km, under the northeastern part of the Paraná basin, which was interpreted as the fossil remnant of the mantle plume responsible for the continental flood basalt magmatism in the initial stages of the Mesozoic South Atlantic rifting. The depth extent of the fossil plume implies that all of the upper mantle has moved coherently with the lithosphere since the breakup of Gondwanaland.

[5] Surface wave dispersion has been used to estimate the average lithospheric structure beneath the network. *Snoke and James* [1997] found high upper mantle *S* wave velocities, in the range 4.6–4.7 km/s, down to at least 100 km. *James and Assumpção* [1996] measured upper mantle anisotropy with SKS splitting showing a pattern of different directions in each geological province: in the São Francisco craton and adjacent Brasília belt the fast anisotropy direction is WNW-ESE; in the western part of the Paraná basin it is SW-NE, while in the central part of the basin (cratonic nucleus) the anisotropy is weak but consistently east-west. These results indicate that the origin of the upper mantle anisotropy is related to the past orogenic processes (''fossil anisotropy'') and not to the current direction of plate movement. This implies that the geological processes observed at the surface involve deformation and tectonic mechanisms encompassing at least part of the upper mantle down to depths as great as 200 km [*Silver and Chan*, 1988, 1991].

[6] In Brazil, little reliable information is available on crustal thickness that could be used to help constrain models of local geological evolution. The worldwide compilation of deep refraction surveys [*Christensen and Mooney*, 1995] shows that the Brazilian lithosphere is one of the least studied in the world. In the absence of seismic information, gravity data alone are commonly used to infer variations of deep crustal structure [e.g., *Blitzkow et al.*, 1979; *Lesquer et al.*, 1981; *Molina et al.*, 1989; *Padilha et al.*, 1992; *Ussami et al.*, 1993; *Chapin*, 1996]. With few constraints, gravity models are highly nonunique, and the interpretations require confirmation from other independent methods, especially with seismic data. For example, the gravity data accross the Goiânia Flexure was interpreted by *Lesquer et al.* [1981] as indicating a thinner crust to the NE toward the São Francisco craton, while *Padilha et al.* [1992] interpreted the crust to be thicker toward the NE. The preliminary results of crustal thickness estimates from receiver functions described below, which favor the interpretation of *Lesquer et al.* [1981], will be helpful in better constraining regional gravity interpretations.

[7] Preliminary results of crustal thickness for some BLSP stations, using receiver functions, were given by *James et al.* [1993]. Here we present a more comprehensive analysis which includes data from additional stations, and we discuss the implications for the isostatic mechanisms.

2. Receiver Functions

[8] Receiver function analysis is a method developed by *Langston* [1977, 1979] for isolating from the recorded signal the effects of local structure (primarily crustal) from other effects

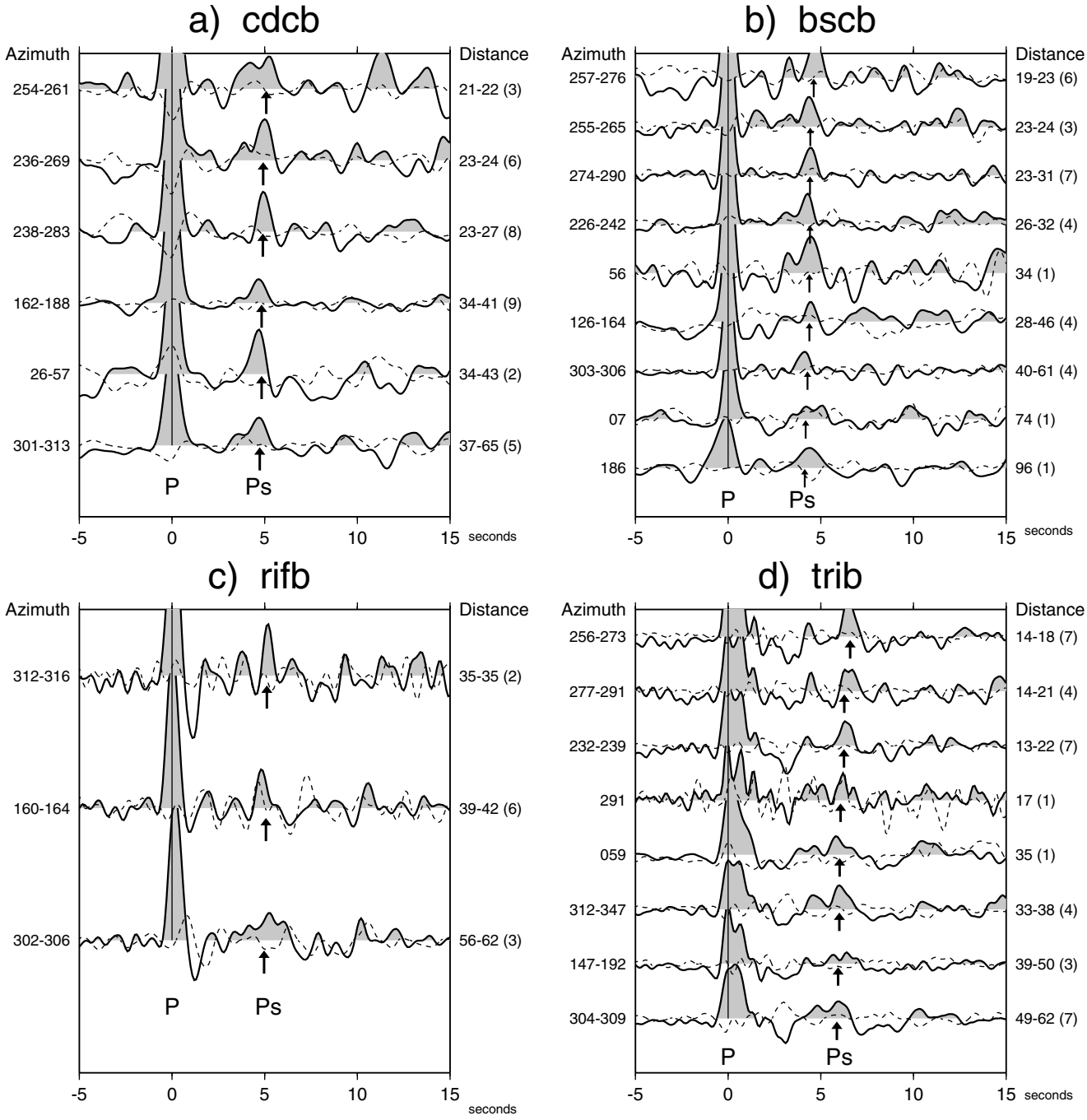

Figure 2. Examples of receiver function stacks for various azimuth and distance ranges. Solid and dashed lines are radial and transverse components, respectively. The arrows mark the expected time of Moho *Ps* conversion for the best crustal thickness. (a and b) Stations cdcb and bscb in the São Francisco craton. (c) Station rifb near the suture zone at the edge of the Paraná basin. (d) Station trib near the axis of the Paraná basin. Numbers on the left are the azimuth ranges (measured at the station) of the events used in each stack; numbers on the right are the distance range with number of traces used in the stack shown in parentheses. The stacks are ordered by average slowness. For station cdcb we used a Gauss filter width $\alpha = 2.0$; for bscb and rifb $\alpha = 3$; for trib we used a higher value, $\alpha = 5$, to show the effect of the sedimentary layers.

due to source complexity and heterogeneity of deeper structures along the propagation path. Langston showed that if the incident *P* waves arrive at a high angle to the surface, deconvolving the vertical component (on which *P* wave energy will dominate) from the horizontal radial component (on which the *SV* waves produced by *P*-to-*S* conversions will be recorded) will yield a deconvolved time series (termed ''receiver function,'' or source equalized trace) on which the major features are *S* wave arrivals related to *P*-to-*S* conversions and reflections in the crust and uppermost mantle beneath the station. *P* wave energy on the radial component that is coherent with energy on the vertical component will be compressed by the deconvolution into a single spike at zero lag time. On the receiver function, all subsequent arrivals after direct *P* have times calculated relative

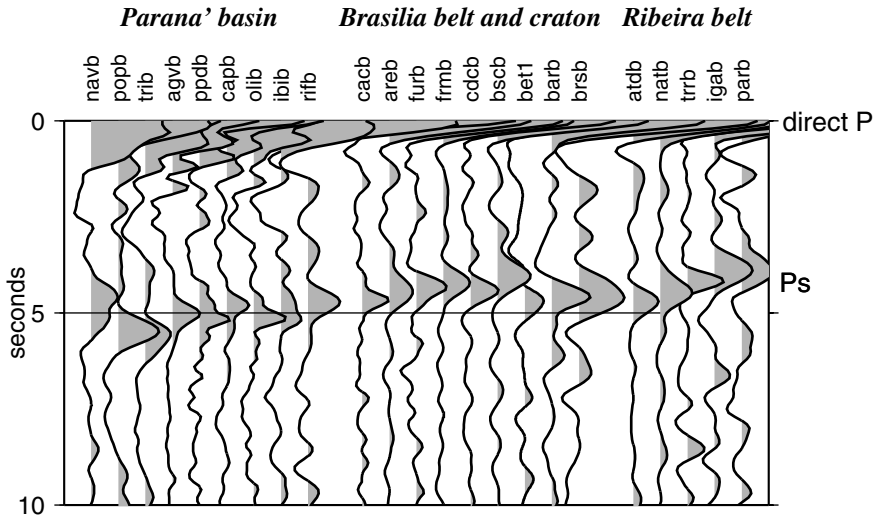

Figure 3. Cross section (roughly west to east) with slant stacked receiver functions. Each receiver function was stacked after correcting the move out of *P*-to-*S* conversions to vertical incidence. Note the *Ps* phase arriving later for the Paraná basin stations compared with stations in the plateau/craton area. Also note the crustal thinning toward the continental margin in the Ribeira belt.

to the coherence peak, so that peak is commonly referred to as the direct *P* wave arrival.

[9] In deconvolving the vertical component from the radial it is necessary to stabilize the spectral ratio by protecting against holes in the vertical component spectrum. This was done by the "trough filler" method where spectral amplitudes lower than a certain threshold ("water level") is replaced by the water level [*Owens et al.*, 1984]. The optimum water level (usually in the range 0.003–0.0001) was chosen for each event. A low-pass Gauss filtering was also used [$\exp(-(\omega^2/4\alpha^2))$] to remove high-frequency scattered energy. Depending on the station the gauss filter width α was set to 2, 3, or 5, which acts as a low-pass filter with corner frequencies at ~0.4, 0.6, or 1.0 Hz, respectively. The frequency content of the receiver functions, however, also depends on other factors, such as the trough filler. The receiver functions have been calculated using routines provided by Charles J. Ammon and include his modifications that preserve amplitude information in the deconvolution.

[10] A crucial feature of the receiver function method is that the source equalized traces for events clustered at roughly the same distance and azimuth can be stacked to improve signal-to-noise ratio. For each station, receiver functions for events with similar back azimuths and distance ranges were stacked. Some examples of receiver functions stacks are shown in Figure 2 for stations cdcb and bscb in the craton, rifb near the suture zone, and trib in the middle of the Paraná basin. The distance ranges and azimuths (measured at the stations) are indicated on the right and left of each trace, respectively. The number of traces used in each stack vary from 1 to 9 and are indicated in parentheses beside the distance range. The transverse component (dashed line) is a useful indication of variations from purely horizontal crustal layerings as well as scattered energy and can be used as a "noise" indication in our case. Even though several features of the radial functions can be well correlated among individual traces, a comparison between the radial and transverse stacks shows that the *P*-to-*S* conversion at the Moho (*Ps* phase) is usually the only phase well above the noise. So the most important information in the receiver function is the *Ps* Moho conversion, which is usually easily identified.

[11] The identification of the Moho *Ps* conversion is made mainly with two criteria: (1) its expected delay of ~5 s with respect to the direct arrival for shield areas where the crust is ~40 km thick and (2) its move out with epicentral distance. The *Ps* converted phase has a move out which depends on the epicentral distance; that is, the time difference *Ps*-*P* decreases with decreasing incidence angle of the *P* wave at the Moho discontinuity. This can be seen in Figure 2, especially for stations with observations within a large distance range. Other phases, such as the surface-reflected *PpPms*, has opposite move out: its delay in relation to the direct *P* increases with epicentral distance and so can be distinguished from the *Ps* conversion. Additionally, synthetic receiver functions are also calculated to confirm the phase identification, as will be seen in section 4.

[12] To produce a single trace per station, we corrected this move out by slant stacking all previous stacks (such as those shown in Figure 2). The slant stacking enhances the *Ps* conversions and reduces other phases, such as *PpPms*, which has opposite move out. The move out correction brings the *Ps*-*P* time to that corresponding to vertical incidence. The amplitudes, on the other hand, are less meaningful now.

[13] A cross section with the final slant stacks for all analyzed BLSP stations are shown in Figure 3. For stations in the Paraná basin, conversions and multiple reflections in the sedimentary layers can be seen following the direct *P* wave for 1 or 2 s; stations outside the basin do not show this pattern. Note also that station rifb is the one with the largest negative trough after the direct *P* wave (Figures 2c and 3), which implies an *S* wave low-velocity zone in the upper crust, as will be seen in section 4. Interestingly, rifb is located right on the postulated "suture zone" of *Lesquer et al.* [1981], as seen in Figure 1.

[14] Stations in the craton and the nearby fold belts show simpler receiver functions with no major features except for the Moho *Ps* conversion. The *Ps*-*P* time is generally smaller for these stations compared with those from the Paraná basin. The stations in the Ribeira belt show a decreasing *Ps*-*P* time toward the coast, which is probably related to the beginning of crustal thinning due to the continent-ocean transition.

3. Velocity Models

[15] Receiver functions can be inverted for the crustal *S* wave velocity profile beneath the station. However, the inversion process is nonlinear and the solution is highly nonunique [e.g., *Ammon et al.*, 1990]. A reliable velocity structure can only be obtained with additional information, such as known velocities of the near surface

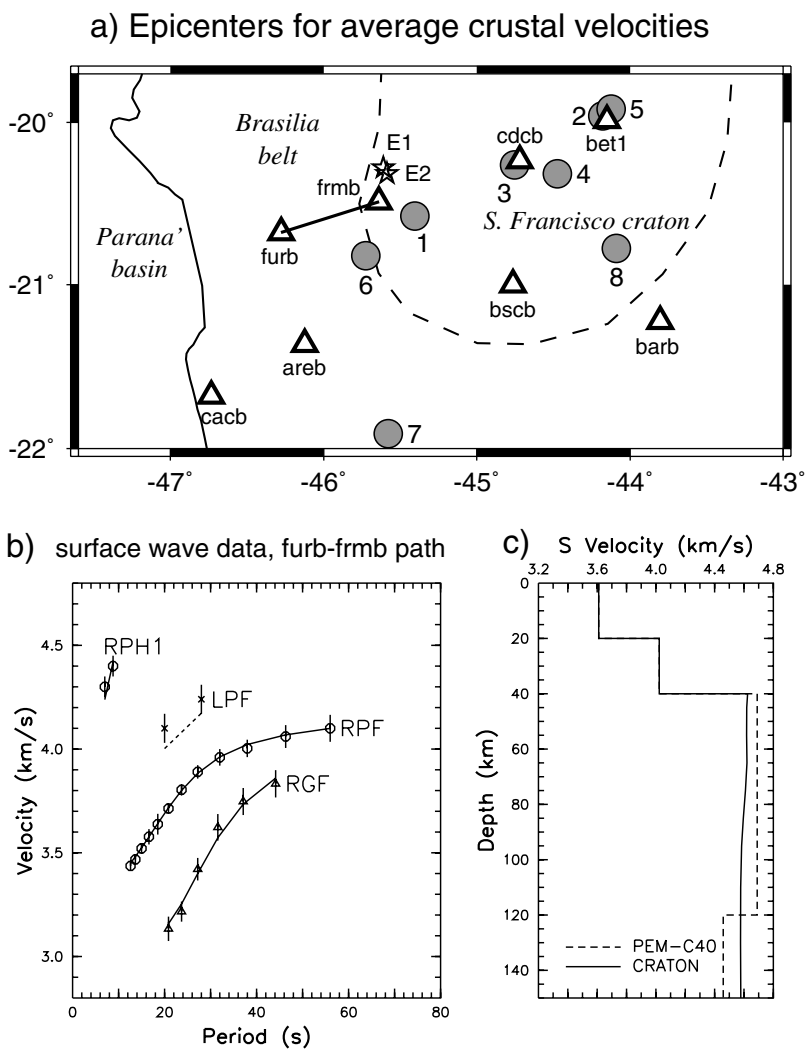

Figure 4. (a) Stations (triangles) and epicenters of local earthquakes (circles) used to estimate an average crustal model for the craton/plateau area. Event numbers are as in Table 1. Stars denote two quarry explosions recorded up to 64 km (Table 2). The line joining stations furb and cdcb is the interstation path used for teleseismic surface wave analysis. (b) Fundamental mode Rayleigh and Love phase velocities (RPF and LPF) and Rayleigh wave group velocities (RGF) determined for one sub-Andean earthquake for the path furb-cdcb. RPH1 is Rayleigh phase velocity for the first higher mode. Symbols with error bars are measured data and lines are calculated curves from the model "CRATON". (c) *S* wave velocity model that fits the dispersion data (solid line) compared with upper mantle velocities of the continental Parameterized Reference Earth Model (dashed line) of *Dziewonski et al.* [1975].

layers. Also, scattered energy from lateral faults or discontinuities can significantly perturb the radial receiver functions [e.g., *Abers*, 1998], so the assumption of horizontal plane layers is questionable. In this paper, we present estimates of crustal thicknesses based on observed time differences between the direct *P* wave and the *Ps* phase, using an average velocity model for the crust, such as was done in the Rocky Mountains by *Sheehan et al.* [1995].

[16] Two models of average crustal velocities were obtained for this study. For the area defined here as "craton/plateau" (São Francisco craton and neighboring Brasília belt) the velocity model was based on analysis of small local earthquakes and one interstation surface wave dispersion curve (Figures 4 and 5). For the Paraná basin, average crustal velocities were based only on surface wave dispersion along two interstation paths from four different teleseisms (Figure 6).

3.1. Craton/Plateau Crustal Model

[17] Several small earthquakes (m_b 2.3–3.7) were well recorded by the BLSP stations in southern Minas Gerais state up to ~300 km distance (Figure 4). Some of these events were also recorded by local stations providing a good estimate of hypocenters and origin times, as indicated in Table 1. In addition, two quarry explosions were timed, and the data up to 64 km were also used. The *P* travel time data, from both first and secondary arrivals, were analyzed to determine an average, first-order velocity-depth model for the region, as follows.

3.1.1. *Vp*/*Vs* ratio. [18] All clear *S* wave arrivals, picked on rotated SH components, indicate an average *Vp*/*Vs* ratio of 1.704 ± 0.003, as shown by the composite Wadati diagram (Figure 5a). This value corresponds to a Poisson ratio of 0.237, significantly below the standard 0.25 value. Although no *Sn*/*Pn* data were used, some secondary arrivals from the lower crust recorded in the distance range 210–275 km, well separated from the *Sn*/*Pn* arrivals, were also included in the Wadati diagram (*P*-*O* times larger than ~35 s). This means the average value of 1.704 for the *Vp*/*Vs* ratio is representative of the whole crust and not only of the upper crustal layers. Good secondary *P* and *S* wave arrivals can be picked with an error less than about ±0.1 and ±0.2 s, respectively,

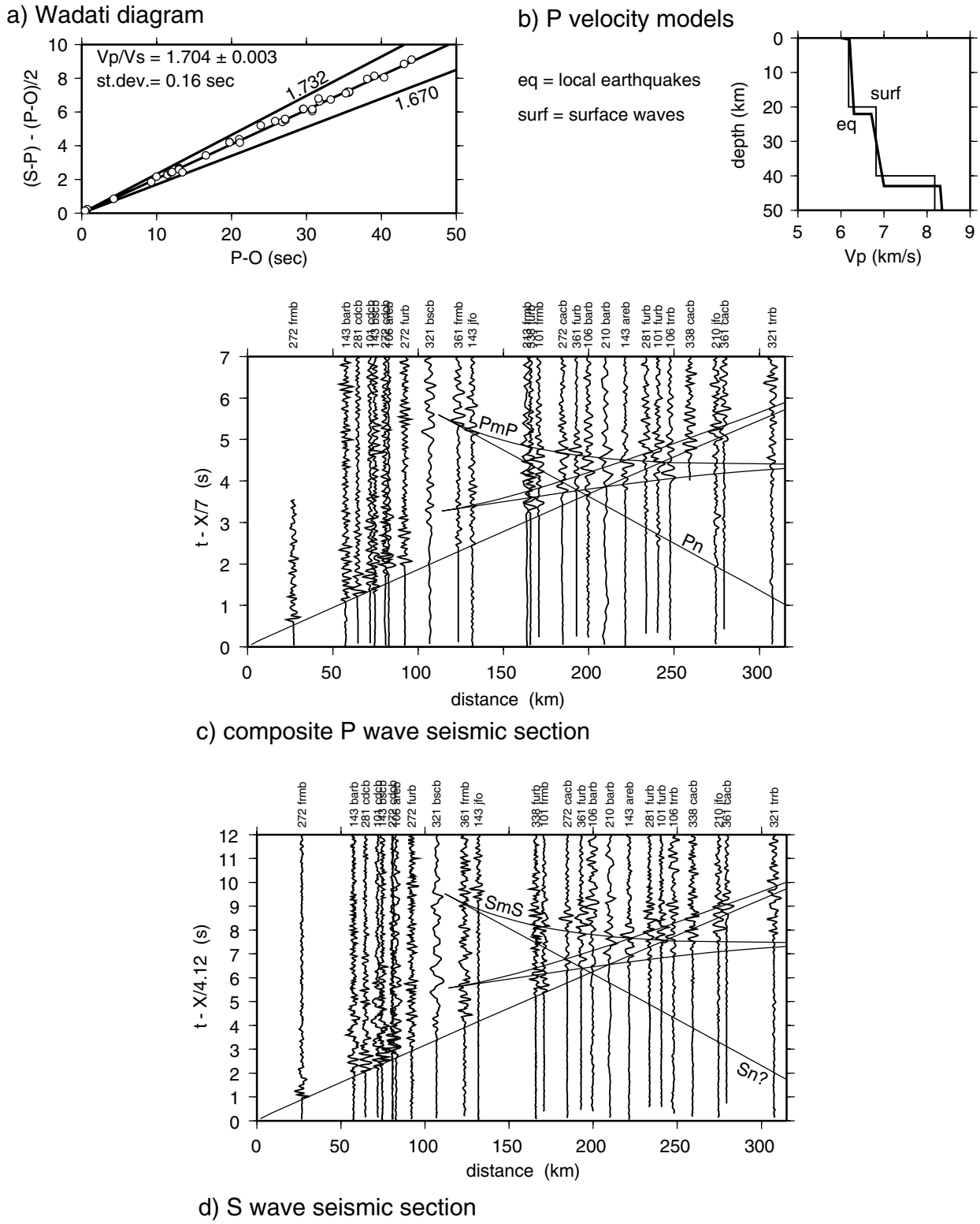

Figure 5. (a) Wadati diagram with sharp *SH* and *P* arrivals showing well-defined *Vp*/*Vs* ratio of 1.704. "Reduced" *S*-*P* values were used to enhance the different *Vp*/*Vs* slopes. The RMS residual in the *S*-*P* times is 0.16 s. The circle radius corresponds to 0.2 s in the vertical (*S*-*P*) axis; most *SH* arrivals have reading uncertainties <0.2 s. (b) *P* wave velocity model that best fits the local earthquake data (eq) compared with the model from surface wave dispersion (surf) between stations furb and frmb (Figure 4c). (c) Composite *P* wave seismic section with travel time curves from model eq. The seismograms were slightly offset to correct for the different hypocentral depths, normalizing the seismic section to zero depth; traces were band-pass filtered 1–7 Hz, and the amplitudes were normalized in the section. *PmP* is Moho reflection, and *Pn* is upper mantle refraction. (d) Composite *S* wave seismic section with travel time curves from model eq. The seismograms were also offset to normalize the times to zero hypocentral depth; traces were band-pass filtered 0.7–4 Hz. Travel time curves are scaled from Figure 5c with a 1.70 *Vp*/*Vs* ratio.

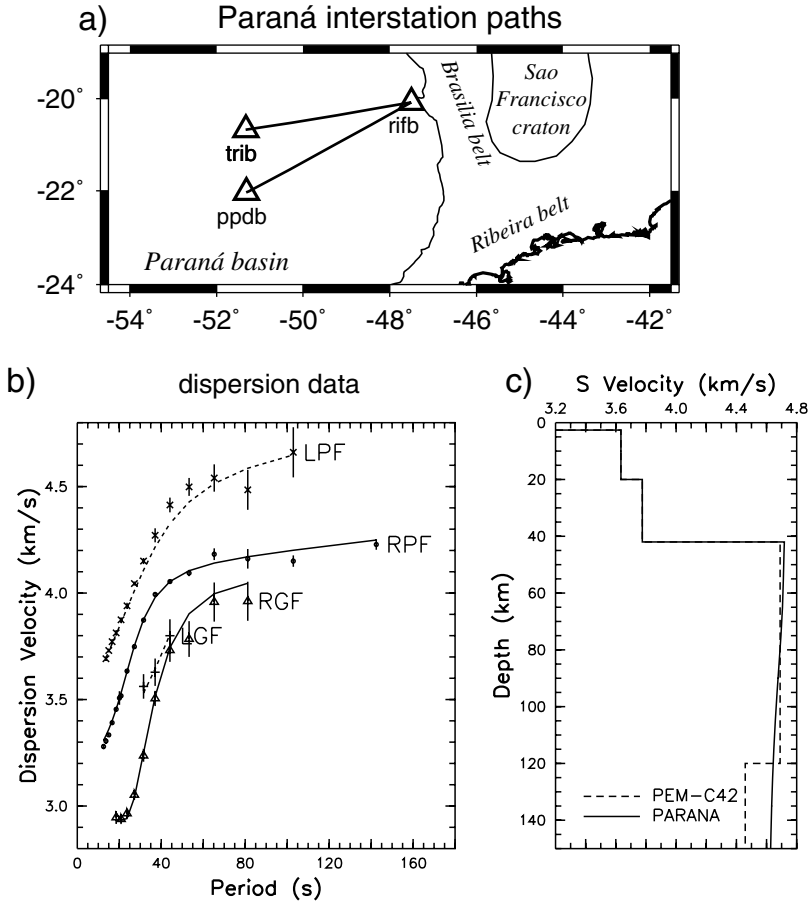

Figure 6. (a) Interstation paths used for teleseismic surface wave analysis in the Paraná basin. Three events were used for ppdb-rifb, and one was used for trib-rifb. Details of the analysis are given by *Snoke and James* [1997]. (b) Dispersion data for the Paraná basin: symbols are as in Figure 4b. (c) *S* wave velocity model obtained with the data for the Paraná basin (solid line labeled PARANÁ) compared with the continental Parameterized Earth Model (dashed line [*Dziewonski et al.*, 1975]) adjusted for a 42 km thick crust.

as seen in the seismic sections of Figures 5c and 5d. At distances >200 km, these picking errors correspond to an uncertainty of only ±0.01 in the *Vp*/*Vs* ratio. A *Vp*/*Vs* ratio lower than the usual 1.73 was consistently observed for all events in different distance ranges, as shown by their individual values in Table 1 (*Vp*/*Vs* column).

3.1.2. *P* wave travel time data. [19] Two sets of *P* wave travel time data were considered: (1) those from events with hypocenters and origin times determined with local data, independently of the regional crustal model, and (2) those from events located with the regional crustal model. The events of data set 1, with more accurate hypocenters (numbers 2, 3, and 5 in Figure 4), were studied in detail by *Assumpção et al.* [1997] and *Assumpção* [1998]. Initially, a preliminary model was defined using data set 1, and this was used to determine the locations of the events in data set 2. A *P* wave record section, corrected for the

Table 1. Local Earthquake Data Used to Estimate Crustal Velocity Structure[a]

Event	Date	Origin Time, UT	Latitude, °S	Longitude, °W	Depth, km	m_b	*Vp/Vs*	Range, km	Locality
1a	9 March 1993	08:56:02.75 (w)	20.577	45.401 (h)	1	3.1	1.70	80–226	Formiga
1b	12 May 1993	00:37:22.96 (w)	20.577	45.401 (h)	1	2.9	1.71	80–226	Formiga
1c	29 Sept. 1993	04:06:27.08 (h)	20.577	45.401 (h)	1	2.5	1.71	27–184	Formiga
2a	1 Aug. 1993	07:56:14.71 (w)	19.959	44.176 (n)	3	2.4	1.67	164–233	Betim
2b	8 Oct. 1993	00:28:04.32 (w)	19.959	44.176 (n)	3	2.6	1.70	64–233	Betim
3	4 Dec. 1993	01:49:57.51 (l)	20.262	44.751 (l)	1	2.6	1.70	4–166	Cajuru
4a	27 Dec. 1993	22:48:10.80 (w)	20.322	44.469 (h)	4	3.5	1.70	122–276	Itaguara
4b	28 Dec. 1993	21:32:06.38 (w)	20.322	44.469 (h)	4	3.2	1.68	122–191	Itaguara
5a	11 Apr. 1994	18:03:20.61 (l)	19.917	44.121 (l)	3	2.5	1.70	3–171	Betim
5b	13 Apr. 1994	00:07:40.61 (l)	19.917	44.121 (l)	3	2.4	1.70	3–171	Betim
6	17 Nov.1997	17:27:01.12 (h)	20.750	45.755 (h)	1	3.7	1.70	78–274	Guapé
7	16 Apr.1998	18:16:44.70 (h)	21.907	45.575 (h)	2	2.3	1.72	83–247	S. Gonçalo
8	23 May 1998	12:48:35.40 (h)	20.776	44.086 (h)	0	2.1	1.70	57–221	L. Dourada

[a] Letters in parentheses are as follows: w, determined by Wadati diagram with sharp *S* and *P* onsets; l, determined with local station; n, determined with local network; h, determined with regional stations and final model.

Table 2. Two-Station Apparent Velocity

Event	Range, km	Apparent Velocity, km/s
Explosion 1	0–23	6.25
Explosion 2	26–64	6.00
5a	3–72	6.31
5a	72–171	6.27
3	4–166	6.20
1c	92–184	6.29
4a	123–192	6.28

hypocentral depth by normalizing all data to zero depth, helped define a better crustal model. Secondary *P* wave arrivals (wide-angle reflections or refractions from lower crust and Moho reflections) were also used to help define the depths to a possible midcrust and to the Moho interfaces. An iterative procedure for relocating the events with the improved model resulted in a final crustal model consistent with all observations, as shown in Figures 5b and 5c. In all models, *Vp*/*Vs* was held fixed at 1.70.

3.1.3. Phase identification. [20] Apparent velocities and incidence angles, which are independent of the crustal model, were also used to help correctly identify the phases. Apparent velocities in the distance range up to 200 km (measured between two stations in roughly the same direction and therefore little affected by hypocentral errors) tend to be in the range 6.0–6.3 km/s as shown in Table 2. The refracted wave from the lower crust could not be identified as first arrival. This suggests a thick upper crust with relatively uniform velocities. In the final model the upper crust was 22 km thick with *P* velocities increasing with depth from 6.0 to 6.3 km/s. Upper mantle refractions (*Pn* waves) are only observed as first arrivals beyond ~200 km. Table 3 shows that the apparent incidence angles at the surface are close to 60° up to 192 km distance. Apparent angles for *Pn* first arrivals and strong secondary arrivals (usually Moho reflections) tend to be in the range 40° to 50°. The data in Table 3 confirm the interpretation that *Pn* refractions are only first arrivals beyond ~200 km, which implies a Moho discontinuity >40 km deep.

[21] Figure 5b shows the resulting velocity model, after three iterations, labeled "eq". The main results were a crustal thickness of 43 km, an average crustal *P* wave velocity of 6.53 km/s (6.1–6.3 km/s for the upper crust and 6.7–7.0 km/s for the lower crust), and a high upper mantle velocity of 8.3 km/s. The average crustal velocity of 6.53 km/s is close to the worldwide average (6.42 ± 0.23) for continental stable areas as compiled by *Christensen and Mooney* [1995]. Velocity gradients for the upper and lower crust were preferred to better model the reflected (secondary) arrivals. *Giese and Shutte* [1975] recorded an unreversed refraction profile in the São Francisco craton, northeast of the study area, from Itabira mine northward. No *Pn* arrivals were recorded by Giese and Shutte, but the Moho reflections suggested a crustal thickness of ~42 km and, possibly, upper mantle velocities of ~8.2km/s, in general agreement with our average model.

[22] The Moho discontinuity in the craton area is well defined by the near critical reflection at 120–130 km distance (*PmP* in Figure 5c), besides the *Pn* head wave. On the other hand, the midcrustal discontinuity is very poorly defined as no strong critical reflections could be identified; an alternative model with a smooth transition between upper and lower crustal velocities would also fit the data. The preferred model (Figures 5b and 5c) has a critical distance for the Moho reflection of 110 km. An estimate of the uncertainty in the average craton model can be obtained by allowing the *PmP* critical distance to vary from 95 to 120 km (the maximum *PmP* amplitude should be close to the critical distance). This range of possible critical distances implies a variation in the crustal average *P* wave velocity from 6.38 to 6.60 km/s, a deviation of ~0.15 km/s from the average 6.53 km/s of the preferred model. Additionaly, during the three iterations of crustal modeling and earthquake relocation process, the average *P* wave velocities did not vary by more than 0.10 km/s.

[23] *Snoke and James* [1994] used surface wave dispersion to estimate the average lithospheric structure beneath the whole BLSP network. Data were insufficient to produce a well-constrained velocity-depth model for the craton alone. A single interstation plateau/cratonic path (furb-frmb) had good quality Rayleigh and Love wave data (including Rayleigh phase velocities for the first higher mode), as shown in Figure 4b. We can use these data to provide a consistency check with the *P* wave refraction results described above. Thus the surface wave data were inverted for crustal and upper mantle velocities using two 20 km thick crustal layers and *Vp*/*Vs* ratios of 1.70 for the crust and 1.78 for the upper mantle. The dispersion data (Figure 4b) are well fit with the model labeled "surf" (Figure 5b). The average crustal *P* velocity for this model is 6.47 km/s, and the *Pn* velocity is 8.24 km/s, consistent with the velocities derived from the local earthquakes. For the surf model the differential *S*-*P* travel time for a ray traveling from the Moho to the surface with normal incidence at the base of the crust is 4.33 s, in agreement with the observed $(Ps\text{-}P)_o$ for stations furb and frmb (Table 4).

[24] The worldwide compilation of lower crust velocities [*Holbrook et al.*, 1992] shows a bimodal distribution for continental stable regions (platforms and shields) with peaks roughly at 6.7–6.8 and 7.2–7.5 km/s. The lower crust velocites found for the plateau area (<7.0 km/s) and the low Poisson's ratio indicate a lower crust composed predominantly of intermediate granulites. Mafic rocks are not likely to be a major constituent of the lower crust in the craton area, which is also consistent with the properties of other Archean crusts, as compiled by *Durrheim and Mooney* [1991]. To estimate the crustal thicknesses from the *Ps*-*P* times of the stations in the craton/plateau, we used a model with two layers of equal thicknesses and velocities of 6.15 and 6.9 km/s. A two-layer model is preferred over a single layer because of the slightly different move out of the *Ps* phase. Thus the adopted two-layer velocity model has an average velocity of 6.5 km/s.

3.2. Paraná Basin Crustal Model

[25] For the Paraná basin, only interstation surface wave velocities were used as no local events were recorded in this aseismic area. Three teleseismic events were analyzed for the path ppdb-rifb and one event for trib-rifb (Figure 6a). Details of the analysis were given by *Snoke and James* [1997], who included three more paths that are omitted here because they traversed parts of the craton as well as the Paraná basin. Weighted averages for both phase and group velocities were determined (Figure 6b) and inverted for a lithospheric velocity model (Figure 6c). Poisson ratios of 0.25 and 0.27 were assumed for the crust and upper mantle, respectively.

Table 3. Observed Apparent Angles *i* at Surface Incidence[a]

Event	Station	Distance, km	Phase[b]	*i*, deg	Arrival
1a	cdcb	81	*Pg*	58	first
1c	furb	92	*Pg*	61	first
4a	frmb	123	*Pg*	62	first
1c	cacb	184	*Pg*?	55	first
4a	furb	192	*Pg*	61	first
5a	furb	240	*Pn*	44	first
4a	cacb	279	*Pn*	51	first
5a	furb	240	*PiP*?	55	second
1c	furb	92	*PmP*?	50	second
4a	frmb	123	*PmP*	49	second
4a	furb	192	*PmP*	40	second
4a	cacb	279	*PmP*?	54	second

[a] Here *i* is taken with respect to vertical. Order is first or secondary arrival.
[b] *Pg*, upper crust arrival; *Pn*, upper mantle refraction; *PmP*, Moho reflection; *PiP*, midcrust reflection.

Table 4. Crustal Thicknesses Derived From *Ps-P* Times[a]

Station Name	Latitude, °S	Longitude, °W	Elevation, km	h_{sed},[b] km	Crustal Thickness, km	$(Ps\text{-}P)_o$,[c] s
			Paraná Basin			
agvb	19.74	50.23	0.45	2.9	43.1 ± 0.9	5.04 ± 0.09
capb	22.81	51.02	0.34	4.5	40.4 ± 1.1	4.82 ± 0.12
ibib	21.78	48.81	0.44	2.8	43.3 ± 1.8	5.07 ± 0.20
navb	21.43	54.18	0.35	3.8	38.8 ± 1.0	4.61 ± 0.12
olib	20.88	48.93	0.48	2.7	43.9 ± 0.8	5.13 ± 0.09
popb	22.46	52.84	0.28	5.0	46.0 ± 2.0	5.47 ± 0.20
ppdb	22.03	51.31	0.30	4.6	43.6 ± 1.3	5.18 ± 0.14
rifb	20.07	47.50	0.86	0.6	41.2 ± 1.5	4.73 ± 0.17
trib	20.67	51.33	0.29	4.3	47.2 ± 1.0	5.57 ± 0.12
			Craton/Plateau			
areb	21.36	46.12	0.98	...	41.2 ± 0.8	4.44 ± 0.08
barb	21.22	43.80	1.14	...	42.3 ± 0.2	4.56 ± 0.02
bet1	19.99	44.15	0.85	...	43.0 ± 0.7	4.64 ± 0.08
brsb	22.54	45.59	1.85	...	42.8 ± 1.8	4.61 ± 0.20
bscb	21.00	44.76	0.96	...	37.5 ± 1.0	4.04 ± 0.11
cacb	21.68	46.73	1.38	...	43.4 ± 0.5	4.67 ± 0.06
cdcb	20.24	44.72	0.86	...	41.5 ± 1.1	4.47 ± 0.12
frmb	20.49	45.64	0.78	...	38.6 ± 1.2	4.16 ± 0.13
furb	20.68	46.28	0.85	...	40.0 ± 0.3	4.30 ± 0.04
			Ribeira Belt			
atdb	21.29	42.86	0.55	...	41.7 ± 0.7	4.68 ± 0.08
igab	23.25	46.11	0.68	...	34.9 ± 1.3	3.92 ± 0.14
parb	23.34	45.62	0.77	...	35.0 ± 0.7	3.94 ± 0.08
natb	21.06	42.00	0.40	...	39.7 ± 1.4	4.47 ± 0.16
trrb	22.15	43.20	0.22	...	38.1 ± 1.3	4.28 ± 0.15

[a] Uncertainties are standard deviations of the various azimuth/distance bins.
[b] Here h_{sed} is thickness of sedimentary layers of the Paraná basin.
[c] $(Ps\text{-}P)_o$ is travel time difference for vertical incidence.

Crustal thickness was taken as 42 km, and the thickness of the lower crustal layer was taken to be 22 km. Drill log data [e.g., *Molina et al.*, 1989] have been used to estimate an average sedimentary section for the Paraná basin 2.6 km thick, with Vp = 4.9 km/s, Vs = 2.7 km/s, and density of 2500 kg/m^3. The resulting model shows an average crustal S wave velocity of 3.71 km/s (excluding the thin sedimentary layer) and a high-velocity mantle lid of ~4.72 km/s. The observed average S wave velocity for the crust of 3.71 km/s corresponds to a Vp of 6.4 km/s for a Vp/Vs ratio of 1.73. The differential S-P travel time for this model for a ray traveling from the Moho to the surface with normal incidence at the base of the crust is 4.91s, which compares well with the average $(Ps\text{-}P)_o$ of 4.98 ± 0.10 S observed at the stations used in the surface wave analysis.

[26] In determining the crustal thicknesses for stations in the Paraná basin from the *Ps-P* times a three-layer model was used with velocities according to the surface wave results. The sedimentary layer had Vp = 4.9 km/s and thickness as in Table 4; the upper crust (Vp = 6.3 km/s) was assumed to reach 20 km depth for all stations; the thickness of the lower crust (Vp = 6.5 km/s) was found from the *Ps-P* time.

[27] For the coastal Ribeira belt, no information is available yet on average crustal velocities. The crustal thicknesses were estimated assuming an average Vp velocity of 6.5 km/s and a Poisson ratio of 0.25. No sedimentary layer was used as all stations were directly on basement rocks.

4. Receiver Function Modeling

[28] Receiver functions inversions were done to test our identification of the Moho *Ps* conversion as well as to check the average model used in estimating crustal thicknesses. Some representative examples are shown in Figure 7. Synthetic receiver functions were calculated for a starting model (craton or Paraná) with the crust and upper mantle consisting of several thin horizontal layers. Perturbations in the layer velocities were calculated with the inversion technique of *Ammon et al.* [1990]. Forward modeling was also carried out by varying the depth of the Moho discontinuity as well as the Vp/Vs ratio (held constant for all layers) to better fit the multiple reflection *PpPms*. Detailed modeling of all features of the receiver function is not necessary as the purpose here is only to determine the compatibility of the average model with the main features of the receiver functions.

[29] Figure 7a shows model results for station cdcb in the São Francisco craton using a stacked receiver function from a NW azimuthal bin. A Vp/Vs ratio of 1.70 (as determined in Figure 5a) was used for the whole crust. Note that the main features of the receiver function can be explained with a crustal model having an average velocity close to the craton model (labeled "earthq." in the top plot of Figure 7a). This modeling shows that the *Ps* phase was correctly identified and that the average P and S wave velocities of the craton model are consistent with the observed receiver functions.

[30] Figure 7b shows model results for station trib in the middle of the Paraná basin. A Vp/Vs ratio of 1.732 (Poisson ratio 0.25) was assumed. The starting model had a sedimentary layer 4.3 km thick (see Table 4) and crustal velocities taken from the surface wave studies. In this example we allowed the inversion process to fit the receiver function in more detail, which resulted in a more complex velocity model. A lower crust discontinuity near 35 km depth seems to be required to explain the peaks preceding the Moho *Ps* and *PpPms* phases. Although this model has a transitional Moho, it has an average crustal velocity and crustal thickness consistent with the Paraná model.

[31] Figure 7c shows model results for station rifb, at the margin of the Paraná basin, close to the suture zone. The trough following the direct P has been modeled as a low-velocity layer in the upper crust. Instabilities in the deconvolution can cause negative troughs near the "P" peak. This effect, however, is usually seen as negative

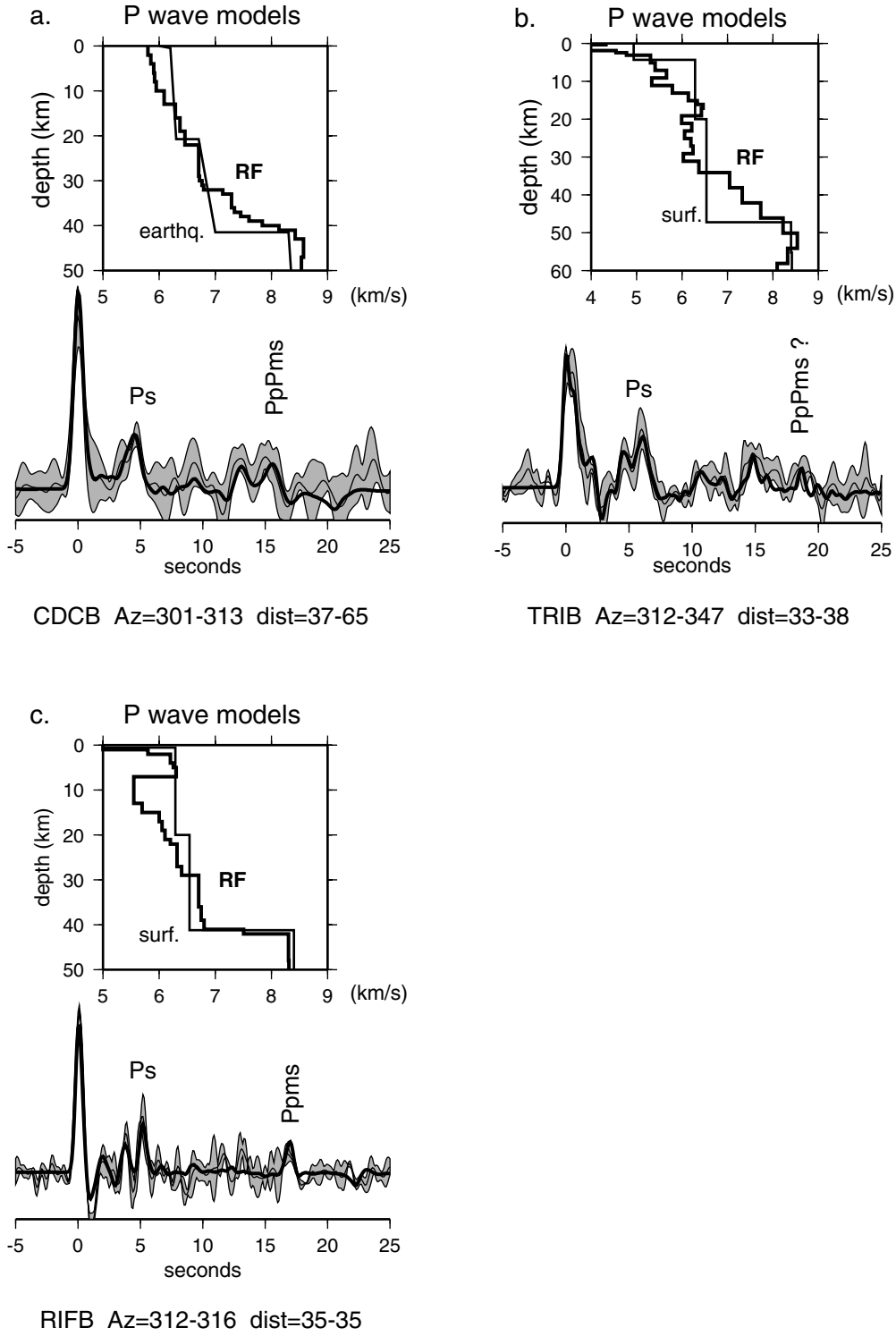

Figure 7. Examples of receiver function modeling for stations (a) cdcb, (b) trib, and (c) rifb. The top plot shows the initial velocity model (thin line) and the model used for the synthetic trace (thick line). The bottom plot shows the synthetic receiver function (thick line) and the observed stacked trace with one standard deviation bounds shaded.

troughs on both sides of the *P* peak, which is not the case here. In addition, all receiver functions had the best trough filler selected to minimize such effects, so we believe the large negative trough following the *P* peak at rifb is a genuine structural signal produced by a low *S* wave velocity zone in the upper crust. The phase 17 s after the direct *P*, tentatively identified as the *PpPms* phase, implies a crustal average *Vp*/*Vs* ratio of 1.71, closer to the craton value than to the assumed 1.73 of the Paraná model. The estimated crustal thickness, however, is very similar to the one given by the initial Paraná model.

[32] Synthetic receiver functions calculated for other stations confirm the identification of the Moho *Ps* conversion. More detailed

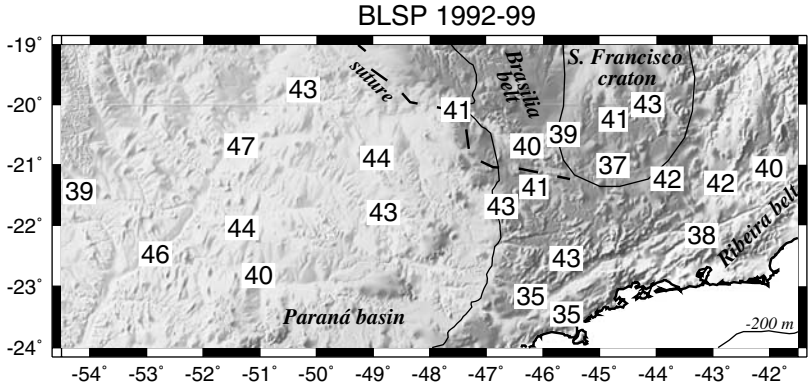

Figure 8. Crustal thicknesses (km) estimated from *Ps-P* times. Shadings denote topography with illumination from the NW. Note thicker crust for the Paraná basin compared with the plateau area. Thin lines show the border of the Paraná basin and approximate limits of the São Francisco craton; thick dashed line is the suture inferred from gravity modeling by *Lesquer et al.* [1981].

modeling of each station would be justified only if lateral variations were taken into account as well as other information such as surface wave dispersion data specific for the area near each station.

5. Results of Crustal Thicknesses

[33] The resulting crustal thicknesses, estimated with the average velocity models, are presented in Table 4 and Figure 8. Table 4 also lists the *Ps-P* time corrected to vertical incidence ($(Ps\text{-}P)_o$ column), which can be used in future refinements when more detailed velocity information becomes available or to constrain tomographic studies such as done by *Van der Lee et al.* [2001]. Crustal thicknesses from 35 to 47 km were obtained. It is clearly seen that the craton/plateau area has a thinner crust than the Paraná basin. Crustal thinning toward the continental margin can also be noted for the stations in the Ribeira belt. It should be noted that the larger crustal thicknesses in the Paraná basin (43 km on average), compared with the craton/plateau area (41 km), were obtained with a lower average *Vp* and higher Poisson ratio; if the same velocity model had been used for both craton/plateau and Paraná basin areas, then the differences in the average thicknesses would be nearly 2 km larger.

[34] The uncertainties in the crustal thicknesses and $(Ps\text{-}P)_o$ shown in Table 4 are the standard deviations from the values of the various stacks for different azimuth and slowness bins and so reflect deviations of the local crustal structure from horizontal layering not uncertainties in the mean crustal thickness beneath the station. To estimate the uncertainties of the mean crustal thickness beneath each station, we need to consider uncertainties in the average crustal *P* and *S* wave velocities. If the average crustal *P* wave velocity can vary by ±0.2 km/s (the standard deviation of the global compilation of *Christensen and Mooney* [1995]), the estimated uncertainty for a 42 km crustal thickness will be around ±1.0 km. An additional uncertainty of ±0.03 in the *Vp*/*Vs* ratio corresponds to an uncertainty of ±1.6 km in the crustal thickness. So the total uncertainties in the mean crustal thicknesses listed in Table 4 could be around ±2.5 km, especially for the Paraná and Ribeira belt. For the stations in the craton/plateau area, where a greater control on the average crustal velocities is available (especially the *Vp*/*Vs* ratio), the uncertainties are smaller. The combined uncertainties of ±0.15 km/s of the average *P* wave velocity and ±0.01 in the *Vp*/*Vs* ratio lead to a total uncertainty of about ±1.6 km in the crustal thicknesses for the craton/plateau area.

[35] In SE Brazil the region of higher topography (Serra da Mantiqueira plateau, southern part of the craton and surrounding fold belt, Figure 1) is characterized by lower Bouguer anomalies (Figure 9a), indicating that regional isostasy is maintained. In the low-elevation area of the Paraná basin, crustal thicknesses vary from 39 to 47 km, while in the plateau the crust is usually thinner (37–43 km) as seen in Figures 8 and 9b. This is the opposite pattern one would expect if isostasy were achieved mainly by varying crustal thickness, as often assumed in gravity modelings of crustal structure. Bouguer anomalies used here were taken from *Ussami and Sá* [1993] and *Ussami et al.* [1993] and are accurate to within 1 mGal.

[36] If the average densities for the crust and for the upper mantle are assumed constant in the study region, then Bouguer anomalies could be calculated from the elevation and crustal thickness, as shown in Figure 9c, where a crust-mantle density contrast of 400 kg/m^3 was used. Because the calculated and observed gravity have no correlation, we must conclude that isostasy is achieved mainly by density variations. So either the crust or the upper mantle in the Paraná basin has higher density compared with the São Francisco craton and Brasília belt.

[37] Figure 10a summarizes the average topographic elevations and crustal thicknesses found for the Paraná basin and the craton area. For the craton area the average values were obtained with stations bet1, cdcb, bscb, and frmb (all in the craton itself) and furb in the nearby fold belt. Although furb is not directly located in the exposed cratonic block, the little deformed, low-grade metasediments in the area and the high upper mantle velocities found in the tomographic studies [*VanDecar et al.*, 1995] suggest a cratonic basement little affected by the Brasiliano orogeny. We excluded from the averages used in Figure 10 the stations close to the Brasiliano suture (rifb, cacb, areb, and brsb) where a thick crust could have originated by crustal shortening during the collision. Also, flexural effects near the suture [*Lesquer et al.*, 1981] prevent simple gravity calculations when analyzing the relations between elevation, gravity, and crustal thickness.

6. Discussion

[38] Two end-member models can be considered to make the crustal thicknesses compatible with isostasy requirements: (1) lower-density lithospheric mantle in the craton area or (2) higher crustal density in the Paraná basin. For each hypothesis, we calculated the densities in two ways: matching the difference in the Bouguer anomalies between Paraná basin and craton (20 mGal) and balancing the total weight of the lithospheres (assuming a depth of compensation of 150 km). The average crust in the Paraná basin was modeled with three layers: a sedimentary layer with fixed *Vp* = 4.9 km/s, density of 2500 kg/m^3 (values

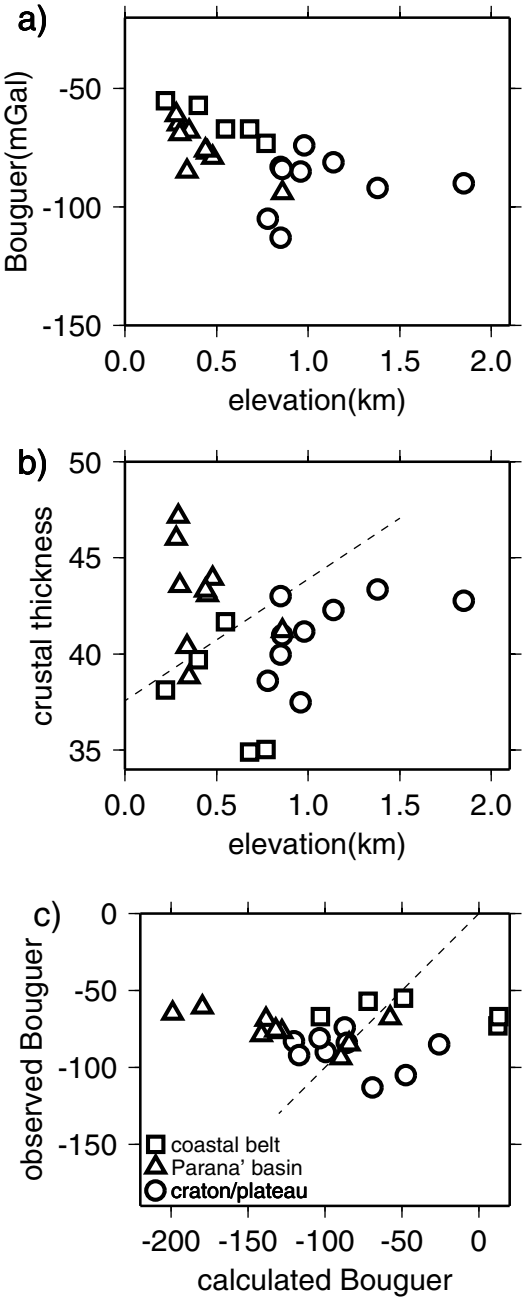

Figure 9. Comparisons between Bouguer anomalies, station elevations, and crustal thicknesses for the BLSP stations sites. (a) Bouguer anomalies and elevations. Higher elevations tend to have more negative Bouguer anomalies, as expected from isostasy. (b) Crustal thicknesses and elevations: sites at higher altitudes in the plateau tend to have thinner crust, contrary to what would be expected from Airy isostasy (dashed line). (c) Observed and calculated Bouguer anomalies, assuming no lateral variations of crustal and mantle densities. Note lack of correlation between observed and calculated values indicating differences in crustal (or mantle) densities between the basin and the plateau. Observed Bouguer anomalies are from *Sá et al.* [1993] and *Ussami and Sá* [1993].

from *Molina et al.* [1989]), and thickness of 3.7 km (average of the stations used in th gravity analysis); an upper crust with fixed *P* wave velocity of 6.29 km/s down to 20 km depth; and a lower crust with velocity-density to be modeled. We used the *P* wave velocity-density relations recommended by *Christensen and Mooney* [1995], such as

$$\rho = 5141 - 14539/V_p,$$

valid for a depth of 30 km and used for the lower crust.

6.1. Low Density in the Craton Lithosphere

[39] Assuming that the craton and the Paraná crusts have the same *P* wave velocities and densities, the lithospheric mantle in the craton has to be less dense than the lithospheric mantle beneath the Paraná basin. A difference of -30 kg/m^3 or -40 kg/m^3 is necessary to match the 20 mGal Bouguer difference or the weight of the lithospheres, respectively. This is in general agreement with the model of *Hawkesworth et al.* [1990] for a depleted ($\sim$1% lower FeO), more buoyant (-30 kg/m^3) Archean lithosphere compared to the Proterozoic lithosphere. Although the lithospheric mantle beneath the craton has a lower density, its *P* wave velocity is still normally high, as suggested both by the 8.3 km/s *Pn* velocity of the craton model above and by the upper mantle tomography results of *VanDecar et al.* [1995]. Because the relation between *P* wave velocity and density depends on the mean atomic number of the rock constituents [*Birch*, 1961; *Chung*, 1972], a depleted upper mantle (low FeO) is consistent with a lower density but still high velocity. A thinner crust and more buoyant, depleted upper mantle for the Archean lithosphere is also consistent with *Durrheim and Mooney*'s [1991] model of crustal evolution.

6.2. High Crustal Density Beneath the Paraná Basin

[40] As an alternative hypothesis, we examine models in which we assume a more mafic, higher-density lower crust beneath the Paraná basin but where crustal velocity structure is constrained by the observed *Ps-P* lapse times (Table 4). In the velocity-density equation above, higher densities imply higher *P* wave velocities, so that a more dense lower crustal section beneath the Paraná basin would in turn require an increase in calculated crustal thickness for a given *Ps-P* lapse time. The increase in calculated crustal thickness due to a higher velocity crust is offset in that the mafic rocks likely to be major constituents of the lower crust have relatively high Poisson's ratios, commonly in the range 0.27–0.30 [*Holbrook et al.*, 1992]. A high Poisson's ratio (i.e., high *Vp*/*Vs* ratio) leads to a decreased crustal thickness for a given *Ps-P* lapse time. In the following examples, we model the crust beneath the Paraná basin assuming a Poissons ratio of 0.28 for the sedimentary layer, 0.25 for the upper crust, and 0.29 for a predominantly mafic lower crustal layer. The above velocity-density relationship is used to relate the density and *Vp*. The upper mantle is assumed to have a uniform density of 3400 kg/m^3.

[41] Given these assumptions and constraints, we get the following results: (1) to produce the 20 mGal Bouguer anomaly contrast requires a density increase of 130 kg/m^3, with an implied *Vp* = 7.1 km/s; (2) to balance the lithosphere weights requires a density increase of 190 kg/m^3, with an implied *Vp* = 7.3 km/s. On the basis of these revised velocity calculations the total crustal thickness decreases by 1.1 or 0.5 km, respectively. The high *P* wave velocities and the high Poisson's ratio in the lower crust yield an average crustal *S* wave velocity of $\sim$3.8 km/s, still compatible with the surface wave results (average of 3.7 km/s).

[42] *Durrheim and Mooney* [1991] show that Proterozoic crusts are often characterized by high *P* wave velocity (*Vp* > 7.0 km/s) in the lower crust, which they interpreted as being most probably due to rocks with gabbro to olivine-gabbro bulk composition. This predominantly mafic composition corresponds to the high velocity peak (*Vp* 7.0–7.5 km/s) found in the compilations of lower crustal structure by *Holbrook et al.* [1992]. The favored mechanism for the origin of a Proterozoic mafic lower crust is basaltic underplating [*Hawkesworth et al.*, 1990; *Durrheim and Mooney*, 1991]. In the middle of the Paraná

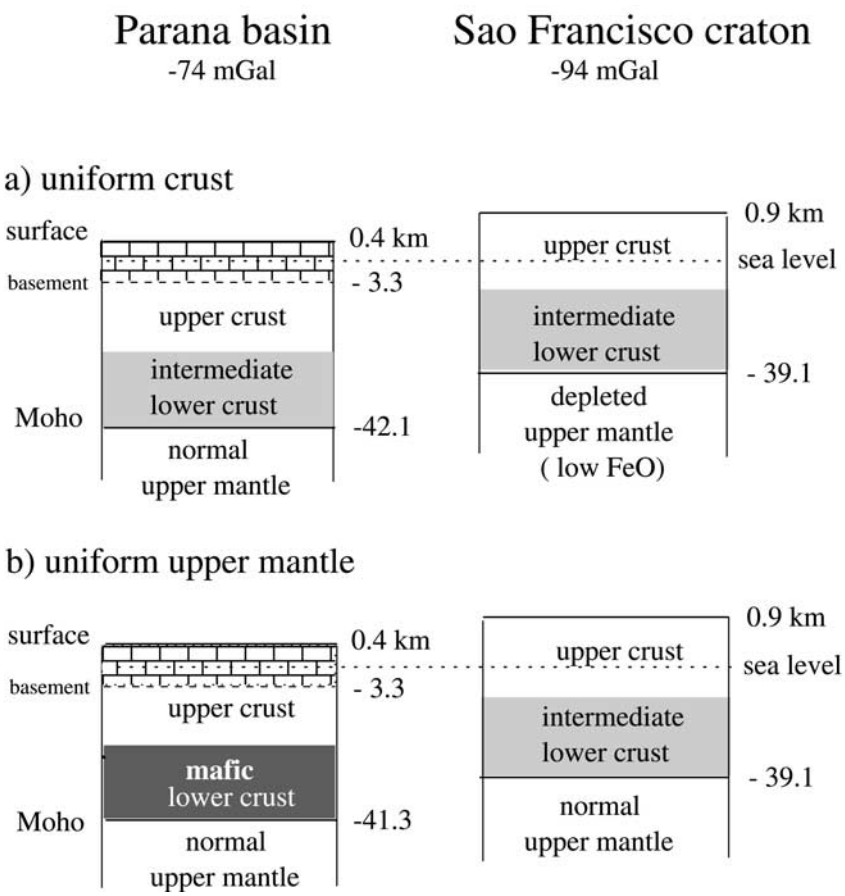

Figure 10. Comparison of average crustal values between Paraná basin and São Francisco craton. Numbers to the right of each column are elevations and depths below sea level (km), not to scale. (a) Uniform crust, with average thicknesses according to Table 4. If both crustal sections have the same density, the craton lithospheric mantle must have lower density such as caused by depleted composition. (b) Uniform upper mantle. If both lithospheric mantle sections have the same density, the crust beneath the Paraná basin must have higher density, such as caused by a mafic lower crust, in which case its thickness as calculated from the receiver functions will be slightly reduced.

basin, *Molina et al.* [1989] modeled variations in the Bouguer and free-air anomalies as due to a high-density lower crust, also attributed to underplating. In the case of the Paraná basin, underplating could have occurred both during the Proterozoic formation of the original crust and during the massive extrusion of the Mesozoic basalt flows, just prior to the South Atlantic opening. In fact, an important extensional event in the Paraná basin at 296 Ma [*Quintas et al.*, 1999] produced maximum subsidence rates in the middle of the basin near stations trib, ppdb, and popb. It is plausible that a weakened lithosphere in this region favored the later basalt flow magmatism (at 140 Ma) with accompanying underplating in the lower crust.

7. Conclusion

[43] Clearly, simple estimates of crustal thicknesses based on *Ps-P* times cannot uniquely define detailed evolutionary models for crustal evolution. The two end-member models presented above are both consistent with Archean/Proterozoic crustal evolution as suggested by *Hawkesworth et al.* [1990] and *Durrheim and Mooney* [1991]. Probably both depleted (buoyant) Archean lithosphere and underplated (more dense) Proterozoic lower crust, to a lesser degree than the values above, could occur in southeastern Brazil.

[44] On the other hand, the results presented here can be helpful in better constraining crustal models derived mainly from gravity data. For example, in modeling the suture zone between the Paraná basin and the São Francisco craton, *Lesquer et al.* [1981] used a slightly thicker crust (and 70 kg/m^3 more dense) beneath the Paraná basin compared with the craton, which is in general agreement with our results. On the other hand, *Padilha et al.* [1992] modeled the same suture, near station AGVB, with the crust beneath the Paraná basin up to 5 km thinner than in the fold belt, which is less likely to be valid in view of the data presented here. *Ussami et al.* [1993] and *Chapin* [1996] calculate isostatic gravity anomalies in South America assuming topography is compensated by crustal thickening. While this may be valid for comparing large, diverse areas, such as Andes and stable platform, it is not a valid hypothesis to be used within the SE Brazil platform. The *Ps-P* times and estimates of crustal thicknesses presented here should help constrain future models of crustal structure in SE Brazil.

[45] **Acknowledgments.** This experiment involved the valuable collaboration of the following institutions in Brazil: IPT, CESP, UNESP (Pres. Prudente), CEMIG, and FURNAS. We specially thank Randy Kuehnel (Carnegie), Luis Carlos Ribotta (IPT), and José Roberto Barbosa (IAG) for their efforts and responsibilities during field work. The receiver function code was kindly provided by Charles Ammon; the surface wave inversion program (SURF) was written by Bob Herrmann. Map plots were done using GMT [*Wessel and Smith*, 1991]. Work carried out with support from Brazilian agencies PADCT (grants 65.93.0402 and 62.0442/94-8), FAPESP (90/03741-5 and 97/03640-6), and CNPq (30.6227/79) and from the U.S. NSF (EAR-9304503).

References

Abers, G. A., Array measurements of phases used in receiver-function calculations: Importance of scattering, *Bull. Seismol. Soc. Am.*, *88*, 313–318, 1998.

Ammon, C. J., G. E. Randall, and G. Zandt, On the nonuniqueness of receiver function inversions, *J. Geophys. Res.*, *95*, 15,303–15,318, 1990.

Assumpção, M., Focal mechanisms of small earthquakes in SE Brazilian shield: A test of stress models of the South American plate, *Geophys. J. Int.*, *133*, 490–498, 1998.

Assumpção, M., J. R. Barbosa, J. Berrocal, A. Bassini, J. A. V. Veloso, V. Mârza, M. Huelsen, and L. C. Ribotta, Seismicity patterns and focal mechanisms in SE Brazil, *Rev. Bras. Geofís.*, *15*, 119–132, 1997.

Birch, F., The velocity of compressional waves in rocks to 10 Kbars, part 2, *J. Geophys. Res.*, *66*, 2199–2224, 1961.

Blitzkow, D., M. Mantovani, P. Gasparini, and N. C. Sá, Crustal structure of SE Minas Gerais deduced from gravity measurements, *Rev. Bras. Geociênc.*, *9*, 39–43, 1979.

Brito Neves, B., and U. Cordani, Tectonic evolution of South America during the Late Proterozoic, *Precambrian Res.*, *53*, 23–40, 1991.

Chapin, D. A., A deterministic approach towards isostatic gravity residuals—A case study from South America, *Geophysics*, *61*, 1022–1033, 1996.

Chung, D. H., Birch's law: Why is it so good?, *Science*, *177*, 261–263, 1972.

Christensen, I., and W. D. Mooney, Seismic velocity structure and composition of the continental crust: A global view, *J. Geophys. Res.*, *100*, 9761–9788, 1995.

Cordani, U. G., B. B. Brito Neves, R. A. Fuck, R. Porto, A. T. Filho, and F. M. B. Cunha, Estudo preliminar de integração do pré-Cambriano com os eventos tectônicos das bacias sedimentares brasileiras, *Rev. Ciênc. Técnica Petróleo15*, Petrobrás, Rio de Janeiro, Brazil, 1984.

Durrheim, R. J., and W. D. Mooney, Archean and Proterozoic crustal evolution: Evidence from crustal seismology, *Geology*, *19*, 606–609, 1991.

Dziewonski, A. M., A. L. Hales, and E. R. Lapwood, Parametrically simple Earth models consistent with geophysical data, *Phys. Earth Planet. Inter.*, *10*, 12–48, 1975.

Giese, P., and J. Shutte, Preliminary report on the results of seismic measurements in the Brazilian coastal mountains in March/April 1975, 12 pp., Free Univ. of Berlin, Berlin, Germany, 1975.

Hawkesworth, C. J., P. D. Kempton, N. W. Rogers, R. M. Ellam, and P. W. Calsteren, Continental mantle lithosphere, and shallow level enrichment processes in the Earth's mantle, *Earth Planet. Sci. Lett.*, *96*, 256–268, 1990.

Holbrook, W. S., W. D. Mooney, and N. I. Christensen, The seismic velocity structure of the deep continental crust, in *Continental Lower Crust, Dev. in Geotectonics*, vol. 23 edited by D. M. Fountain, R. Arculus, and R. W. Kay, pp. 1–34, Elsevier Sci., New York, 1992.

James, D., M. Assumpção, A. Snoke, L. C. Ribotta, and R. Kuehnel, Seismic studies of continental lithosphere beneath SE Brazil, *An. Acad. Bras. Cienc.*, *65* (Suppl. 2), 227–250, 1993.

James, D. E., and M. Assumpção, Tectonic implications of *S*-wave anisotropy beneath SE Brazil, *Geophys. J. Int.*, *126*, 1–10, 1996.

Langston, C. A., The effect of planar dipping structure on source and receiver responses for constant ray parameter, *Bull. Seismol. Soc. Am.*, *67*, 1029–1050, 1977.

Langston, C. A., Structure under Mount Rainier, Washington, inferred from teleseismic body waves, *J. Geophys. Res.*, *84*, 4749–4762, 1979.

Lesquer, A., F. F. M. Almeida, A. Davino, J. C. Lachaud, and P. Maillard, Signification structurales des anomalies gravimetriques de la partie sud du craton de S. Francisco (Brésil), *Tectonophysics*, *76*, 273–293, 1981.

Molina, E. C., N. Ussami, N. C. Sá, and D. Blitzkow, Interpretação dos dados gravimétricos da parte norte da bacia do Paraná, *Rev. Bras. Geociênc.*, *19*, 187–196, 1989.

O'Connor, J. M., and R. A. Duncan, Evolution of the Walvis ridge-Rio Grande rise hot spot system: Implications for African and South America plate motions over plumes, *J. Geophys. Res.*, *95*, 17,475–17,502, 1990.

Owens, T. J., G. Zandt, and S. R. Taylor, Seismic evidence for an ancient rift beneath the Cumberland plateau, Tennessee: A detailed analysis of broadband teleseismic *P* waveforms, *J. Geophys. Res.*, *89*, 7783–7795, 1984.

Owens, T. J., S. R. Taylor, and G. Zandt, Crustal structure at regional seismic test network stations determined from inversion of broadband teleseismic *P* waveforms, *Bull. Seismol. Soc. Am.*, *77*, 631–662, 1987.

Padilha, A. L., N. B. Trivedi, I. Vitorello, and J. M. Costa, Upper crustal structure of the NE Paraná basin, Brazil, determined from integrated magnetotelluric and gravity measurements, *J. Geophys. Res.*, *97*, 3351–3365, 1992.

Quintas, M. C. L., M. S. M. Mantovani, and P. V. Zalán, Contribuição ao estudo da evolução mecânica da Bacia do Paraná, *Rev. Bras. Geociênc.*, *29*, 217–226, 1999.

Sá, N. C., N. Ussami, and E. C. Molina, Gravity map of Brazil, 1, Representation of free-air and Bouguer anomalies, *J. Geophys. Res.*, *98*, 2187–2197, 1993.

Sheehan, A. F., G. A. Abers, C. H. Jones, and A. L. Lerner-Lam, Crustal thickness variations across the Colorado Rocky Mountain from teleseismic receiver functions, *J. Geophys. Res.*, *100*, 20,391–20,404, 1995.

Silver, P. G., and W. W. Chan, Implications for continental structure and evolution from seismic anisotropy, *Nature*, *335*, 34–39, 1988.

Silver, P. G., and W. W. Chan, Shear-wave splitting and subcontinental mantle deformation, *J. Geophys. Res.*, *96*, 16,429–16,454, 1991.

Snoke, J. A., and D. James, Structure of the crust and upper mantle beneath southern Brazil from surface wave inversion, *Eos. Trans. AGU*, *75*(44), Fall Meet. Suppl., 462, 1994.

Snoke, J. A., and D. James, Lithospheric structure of the Chaco and Paraná basins of South America from surface-wave inversion, *J. Geophys. Res.*, *102*, 2939–2951, 1997.

Teixeira, W., and M. C. H. Figueiredo, An outline of Early Proterozoic crustal evolution in the São Francisco craton, Brazil: A review, *Precambrain Res.*, *53*, 1–22, 1991.

Turner, S., M. Regelous, S. Kelley, C. J. Hawkesworth, and M. Mantovani, Magmatism and continental break-up in the South Atlantic: High precision $^{40}Ar-^{39}Ar$ geochronology, *Earth Planet. Sci. Lett.*, *121*, 333–348, 1994.

Ussami, N., and N. C. Sá, Digital (10′ by 10′) gravity maps of the São Francisco craton and marginal fold/thrust belts, in *Proceedings II Simpósio sobre o craton do São Francisco*, pp. 137–139, Soc. Bras. Geol., Sao Paulo, Brazil, 1993.

Ussami, N., N. C. Sá, and E. C. Molina, Gravity map of Brazil, 2, Regional and residual isostatic anomalies and their correlation with major tectonic provinces, *J. Geophys. Res.*, *98*, 2199–2208, 1993.

VanDecar, J. C., D. E. James, and M. Assumpção, Seismic evidence for a fossil mantle plume beneath South America and implications for plate driving forces, *Nature*, *378*, 25–31, 1995.

Van der Lee, S., D. James, and P. Silver, Upper mantle *S* velocity structure under South America, *J. Geophys. Res*., in press, 2001.

Wessel, P., and W. H. F. Smith, Free software helps map and display data, *Eos Trans. AGU*, *72*(41), 441, 445–446, 1991.

Zalan, P., S. Wolff, J. Conceicao, A. Marques, M. Astolfi, I. Vieira, V. Appi, and O. Zanotto, Bacia do Paraná, in *Origem e Evolução de Bacias Sedimentares Brasileiras*, edited by G. Gabaglia, and G. Milani, pp 135–168, Petrobras, Rio de Janeiro, Brazil, 1990.

M. Assumpção, Institute of Astronomy, Geophysics, and Atmospheric Science, University of São Paulo, Rua do Matão 1226, São Paulo, SP, 05508-900 Brazil. (marcelo@iag.usp.br)

D. James, Department of Terrestrial Magnetism, Carnegie Institution of Washington, 5241 Broad Branch Road, NW, Washington, DC 20015, USA. (james@dtm.ciw.edu)

A. Snoke, Virginia Tech Seismological Observatory, Department of Geological Sciences, Virginia Polytechnical Institute and State University, Blacksburg, VA 24061, USA. (snoke@vt.edu)